Journal of Hydrology 607 (2022) 127480

Contents lists available at ScienceDirect

Journal of Hydrology

journal homepage: www.elsevier.com/locate/jhydrol

Research papers

Nutrient limitations on primary productivity and phosphorus removal by biological carbon pumps in dammed karst rivers: Implications for eutrophication control

Hailong Sun [a], Cuihong Han [a], Zaihua Liu [a,b,*], Yu Wei [a], Song Ma [a,c], Qian Bao [a,c], Yi Zhang [a,c], Hao Yan [a]

[a] State Key Laboratory of Environmental Geochemistry, Institute of Geochemistry, Chinese Academy of Sciences, Guiyang 550081, China
[b] CAS Center for Excellence in Quaternary Science and Global Change, 710061 Xi'an, China
[c] University of Chinese Academy of Sciences, Beijing 100049, China

ARTICLE INFO

This manuscript was handled by Huaming Guo, Editor-in-Chief, with the assistance of Rafael Perez Lopez, Associate Editor

Keywords:
DIC fertilization
BCP effect
Phosphorus removal
N:P stoichiometry
Cyanobacteria abundance
Eutrophication control
Dammed karst rivers

ABSTRACT

Biological carbon pumps (BCPs) convert dissolved inorganic carbon (DIC) into autochthonous organic carbon (AOC), which is the key to form long-term stable carbonate weathering-related carbon sink. The DIC fertilization may increase the strength of BCP. As a phase of BCP, eutrophication is one of the major problems in surface water environments which shows poor water quality with harmful cyanobacteria blooms. It is generally believed that the controlling elements of eutrophication are nitrogen (N) and phosphorus (P), while the controlling elements of BCP also includes carbon (C). Meanwhile P removal by BCPs through the coprecipitation of P with calcite and Fe (III) oxyhydroxide colloids decreases its content in water bodies and prevent water from cyanobacteria eutrophication. In the present study, we examine the seasonal variations of general physiochemical parameters of the surface water, DIC, total N and total P concentrations, chlorophyll concentrations in three karst river-reservoir systems (PZR, PDR and HFR) in Guizhou Province, Southwest China. The phytoplankton community structure dynamics and the settling flux of the total P and P fractions in the settling particulate matter in PZR and HFR were also examined. It was found that: (1) the nutrient limitations of BCPs shifted from C-limitation to N- or P-limitation after the rivers were dammed; (2) P removal by BCPs reduced the total P concentration and increased the stoichiometric N:P ratio in surface waters; (3) P removal by BCPs alleviated the development of eutrophication by decreasing the relative abundance of Cyanobacteria. Our results demonstrate that the damming of a river may shift the nutrient limitation patterns of dammed karst rivers and the P removal by BCP may retard the development of water body into Cyanophyta-type eutrophication. This may have important implications for eutrophication control (i.e., strengthening BCP effect via DIC fertilization) in HCO_3-Ca type surface water, especially in karst areas, which cover about 15% of the world land surface.

1. Introduction

The biological carbon pump (BCP) in inland water bodies (rivers, lakes, and reservoirs) produced by aquatic photosynthesis can convert dissolved inorganic carbon (DIC) into autochthonous organic carbon (AOC) while simultaneously forming carbonates and autochthonous organic carbon (AOC) (Eq. (1), Liu et al., 2018). The AOC produced by BCPs is the key to forming long-term stable carbonate-weathering C sinks (He et al., 2020; Liu et al., 2010, 2018; Liu et al., 2015). Higher DIC concentrations can induce higher primary productivity of aquatic photosynthetic organisms (known as the BCP effect), which is referred to as DIC fertilization (Chen et al., 2017; Hammer et al., 2019; Kragh and Sand-Jensen, 2018; Yang et al., 2016; Zeng et al., 2019). Under higher DIC conditions, an efficient BCP may have the potential to cause eutrophication (Kragh and Sand-Jensen, 2018; Verspagen et al., 2014). Eutrophication, as a particular phase of BCPs, is one of the major problems in surface water environments and results in poor water quality and harmful cyanobacterial blooms (Schindler, 1974; Smith, 2003).

$$Ca^{2+} + 2HCO_3^- \Rightarrow^{BCP} CaCO_3 + x(CO_2 + H_2O) + (1-x)(CH_2O + O_2) \quad (1)$$

* Corresponding author.
E-mail address: liuzaihua@vip.gyig.ac.cn (Z. Liu).

https://doi.org/10.1016/j.jhydrol.2022.127480
Received 15 June 2021; Received in revised form 30 December 2021; Accepted 15 January 2022
Available online 20 January 2022

Generally, eutrophication of freshwater bodies is believed to be limited by P, N, or both N and P (Abell et al., 2010; Conley et al., 2009; Correll, 1998; Paerl et al., 2011, 2016; Schindler, 1977; Schindler et al., 2008, 2016; Smith et al., 2016; Sterner, 2008; Wang and Wang, 2009). On the other hand, C is generally considered to be the limiting nutrient for BCPs, especially in karst aquatic ecosystems (Chen et al., 2017; Liu et al., 2015; Yang et al., 2016; Zeng et al., 2019). It has long been thought that C is unable to limit aquatic photosynthesis in open water of lakes/reservoirs because these water bodies will tap into the atmospheric reservoir of C to overcome these deficiencies (Schindler, 1977). However, CO_2 diffusion in water is a slow process and cannot satisfy the demand for aquatic photosynthesis (Stumm and Morgan, 1981). Several studies have demonstrated the C limitation of phytoplankton photosynthesis (Hamdan et al., 2018; Hein, 1997; Hein and Sand-Jensen, 1997; Riebesell et al., 1993; Verspagen et al., 2014; Van Dam et al., 2018). CO_2 is the favored substrate for aquatic photosynthesis (Verspagen et al., 2014), and its concentration decreases due to the utilization by phytoplankton for photosynthesis and an increase in pH, which changes the balance between all DIC species ($DIC = CO_{2(aq)} + HCO_3^- + CO_3^{2-}$) from CO_2 to bicarbonate (HCO_3^-) and eventually to CO_3^{2-} (Andersen et al., 2019; Schulte et al., 2011). The C limitation of phytoplankton photosynthesis is very important, and a noticeable problem in karst aquatic ecosystems. It is well known that the water in karst basins has higher concentrations of DIC than in nonkarst catchments because of the the rapid kinetics of carbonate mineral dissolution (Liu et al., 2011). But, the dissolved CO_2 concentration is reduced because of the higher pH of the karst waters, and only 1% of the DIC concentration at pH 8.2 (Schulte et al., 2011). Furthermore, high concentrations of Ca^{2+} and HCO_3^- in karst waters can promote calcium carbonate precipitation (Liu et al., 2006), and calcium carbonate produced by BCPs promotes coprecipitation of P in water, leading to the transformation of soluble to insoluble phosphate (PO_4^{3-}) (Corman et al., 2015, 2016; Hamilton et al., 2009; Kleiner, 1988; Murphy et al., 1983; Otsuki and Wetzel, 1972; Walsh et al., 2019). Otsuki and Wetzel (1972) found that>74% of phosphate ion was found to be precipitated with the carbonates. Hamilton et al. (2009) also found that the calcite sedimentation was a major sink for added P, and about half of the added P was removed from the water column. The Fe(III) oxyhydroxide colloids, which are induced by BCPs due to the increasing pH and dissolved oxygen (DO) concentration, can also absorb P to form coprecipitates (Gunnars et al., 2002; Hoffman et al., 2013; Mayer et al., 1982; Stauffer and Armstrong, 1986; Tang et al., 2019; Yuan et al., 2020). Therefore, P removal by BCPs may alleviate eutrophication (Chen and Liu, 2017).

On the other hand, damming for hydropower generation and irrigation impedes the flow of nutrients (including C, P, and N) along river networks, leading to increased nutrient retention (Humborg et al., 1997; Maavara et al., 2014, 2015, 2020; Van Cappellen and Maavara, 2016). Dammed rivers evolve and form their own elemental biogeochemical cycles (Wang et al., 2018). Further, dammed karst rivers are usually canyon reservoirs with high DIC concentrations, pH, and obvious thermal stratification during spring and summer (Wang et al., 2019). Systematic studies on the effects of nutrient limitation on BCP and the role of P removal by BCPs in eutrophication control are still lacking in dammed karst rivers (Bao et al., 2020; Zeng et al., 2019).

In this study, we investigated three river-reservoir systems of the dammed karst rivers (Pingzhai Reservoir [PZR], Puding Reservoir [PDR], and Hongfeng Reservoir [HFR]) in Guizhou Province, Southwest China, from April 2018 to January 2019. We measured the concentrations of HCO_3^-, $CO_{2(aq)}$, total phosphorus (TP), total nitrogen (TN), and chlorophyll-*a* (Chl-*a*) concentrations, and assessed the phytoplankton community structure in the surface waters of rivers and dammed reservoirs. We also determined the total P flux and the chemical fractions of P in sediment traps. Our aims were to investigate the following issues: (1) the dynamics of nutrient limitations on BCPs in rivers and dammed reservoirs, and the underlying mechanism; (2) the role of P removal by BCPs in preventing water bodies from cyanobacterial eutrophication, and the underlying mechanisms.

2. Materials and methods

2.1. Study area

The PZR is a typical canyon-shaped reservoir located on the Sancha River at the source of the Wujiang River (Fig. 1). Water storage in the PZR commenced in 2015. It has a total capacity of 10.89×10^8 m^3 and a mean depth of 50 m (maximum ~ 125 m). The PDR is located downstream of the PZR (Fig. 1) and began storing water in 1963. It has a surface area of 19.25 km^2, a total capacity of 4.2×10^8 m^3, and a mean depth of 15 m (maximum ~ 25 m). The Sancha River Basin (104°54′–106°24′E, 26°06′-27°00′N), situated in the northwest in the Guizhou Province, China, is a typical karst peak-cluster depression region with abundant carbonates (Hou and Gao, 2019; Gao and Wang, 2019). The river basin is controlled by a subtropical monsoon climate, with an annual mean rainfall of 1100 mm concentrated between May and October.

The HFR is located on the Maotiao River, a tributary of the Wujiang River (Fig. 1). The filling of the reservoir was completed in 1960. It has a water surface area of 57.2 km^2, a storage capacity of 5.9×10^8 m^3 at a normal water level, and a mean depth of 10.5 m (max ~ 45 m). The HFR encompasses the North Lake and South Lake, and the dam is in the east. The HFR has five main inflows, i.e., two into North Lake (Maiweng and Maibao Rivers) and three into South Lake (Yangchang, Maxian, and Houliu Rivers). The bedrock consists mainly of carbonate and clastic rocks. The mean annual temperature is 14.1 °C and the mean annual precipitation is 1,200 mm (Chen et al., 2020; Wu et al., 2017).

Three sampling sites within the Pingzhai river-reservoir system (PZA, BXZ and PZ) and two sampling sites in the Sancha River (SCH and YCZ) were investigated. Four sampling sites were investigated within the Puding river-reservoir system (PDA, PDZ, PDM and PD); two sampling sites in the Sancha River were investigated upstream of the reservoir (LC and MC), and one located downstream of the dam (PDX). In the HFR, two sites were located in the South Lake (NH and HW), one in the junction between the North and South Lake (HYD), another site in the North Lake (100 m from the dam) (HF), and two sites in North Lake (BH and TYH). One sampling site was investigated in the Yangchang River (HQQ) upstream of the South Lake (Fig. 1). The general information of the sampling sites are given in Table S1.

2.2. Field monitoring and in-situ titration

Field monitoring was carried out in April, June, August, and October of 2018 and January 2019. The physiochemical parameters of the surface water were measured in the field using a hand-held water quality meter (PONSEL ODEN, France), including temperature (T), pH, electrical conductivity (EC, 25 °C), and DO, with resolutions of 0.01 °C, 0.01, 0.1 μs/cm and 0.01 mg/L, respectively. Instruments were calibrated prior to deployment at pH 4, 7, and 10 and EC of 1413 μs/cm. The DO probe was calibrated using moist saturated air. Because of their instability, DIC concentrations were determined in *situ* by titration using an Aquamerck alkalinity test kit (Merck, Germany) with a resolution of 0.05 mmol L^{-1}; each sample was titrated two or three times (Liu et al., 2007).

2.3. Sample collection and sediment traps

To study the nutrient limitation of BCPs and the P removal by BCP, the DIC concentrations (HCO_3^- and $CO_{2(aq)}$), concentrations of TN and TP, chlorophyll-a (Chl-a) concentration and phytoplankton density in the surface water, and the TP content and phosphorus fractions in the settling particulate matter, need to be determined.

Water samples were collected 0.5 m below the surface. Samples for analyses of major cations and anions were collected in 20 mL acid-

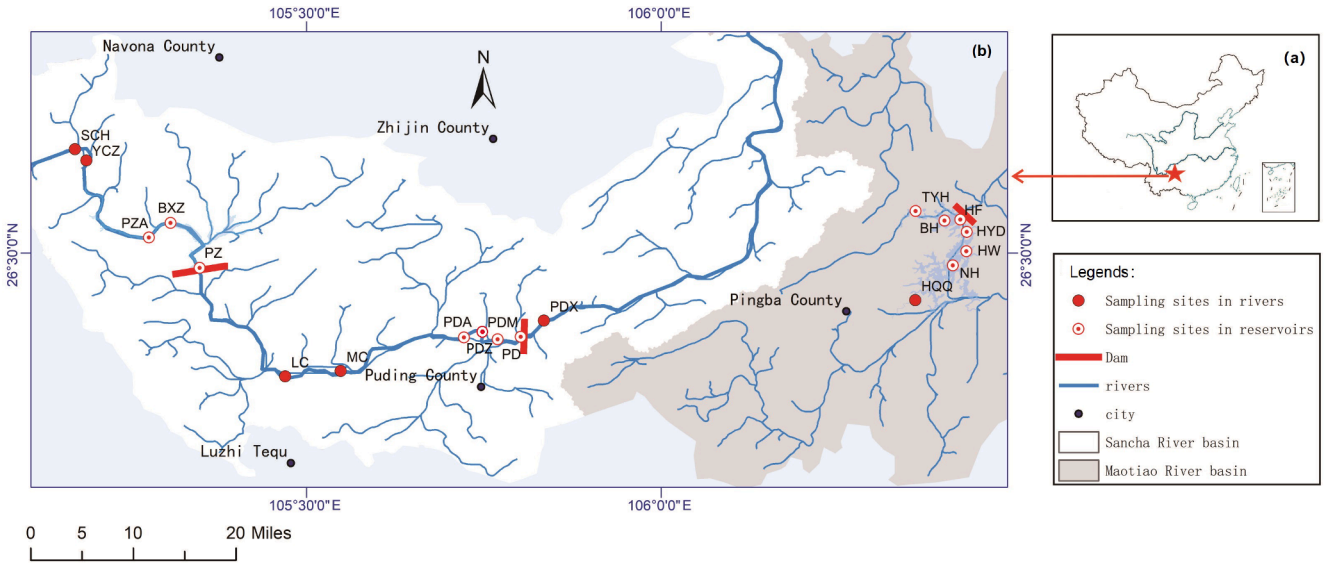

Fig. 1. (a) Study area and (b) sampling sites of the river-reservoir systems, Guizhou province, southwest China.

washed high-density polyethylene bottles using 0.45-μm acetate fiber filters. Samples for cation analyses were acidified to pH < 2.0 using concentrated nitric acid to prevent precipitation and complexation. Samples for TN and TP analyses were stored in 100 mL acid-washed brown glass bottles with Teflon-lined screw caps. All bottles were rinsed three times and the filters were thoroughly flushed with sample water prior to sample collection. After sampling, all bottles were transported to the laboratory and kept away from direct sunlight before storing in the refrigerator, and analyzed at the earliest. Water samples (1 L) were collected and filtered using a 47 mm GF/F filter to determine the chlorophyll-*a* (Chl-*a*) concentration. Phytoplankton samples were collected using a handheld phytoplankton net (64 μm mesh size) in surface waters, and water samples (1 L) were collected for its quantitative analysis. Phytoplankton samples were preserved with Lugol's iodine solution (2% final concentration).

At PZR and HFR, cylindrical sediment traps (length = 1.4 m, diameter = 14 cm) were deployed at PZA, BXZ, PZ, NH, BH, and HF to collect settling particulate matter. The traps were fixed at least 1 m above the sediment surface on ropes held by floats and anchored at the bottom of the reservoirs. The sediment traps were deployed during the period from April 2018 to January 2019. The duration time for collecting settling particulate matter was 2 to 3 months.

2.4. Analysis strategies and calculation of dissolved CO_2 concentrations

Cation concentrations (K^+, Na^+, Ca^{2+}, and Mg^{2+}) were determined by an inductively coupled plasma optical emission spectrometer (Vista-MPX, Varian). Anion concentrations (Cl^-, SO_4^{2-}, and NO_3^-) were determined using an ion chromatography (ICS-90, Dionex) . The experimental minimum detection limit of these ions was 0.01 mg L^{-1}. Chl-*a* concentrations were determined using an ultraviolet spectrometer after extraction in 90% hot alcohol (Pápista et al., 2002). The preserved phytoplankton samples were concentrated to 30 mL. After mixing, 0.1 mL concentrated samples were counted and identified directly using a phytoplankton counting chamber at 400 × magnification.

After freeze-drying, the settling particulates collected by the sediment traps were weighed and passed through a 200 mesh for further analysis. The total P content was determined from dried settling particulate matter using the SMT method (Ruban et al., 2001). The chemical fractions of P were determined using the sequential extraction fractionation described by Hupfer et al. (1995). The following P fractions were extracted: NH_4Cl-P, BD-P, NaOH-SRP, NaOH-NRP, HCl-P, and Res-P. Generally, HCl-P is regarded as a Ca-bound P compound, BD-P is associated with Fe hydroxides (Jensen and Thamdrup, 1993), and NaOH-SRP is the form of P that is bound to metal (mainly Fe and Al) oxides (Kozerski and Kleeberg, 1998).

The dissolved $CO_{2(aq)}$ concentrations were calculated using PHREEQC Interactive 3.4.0 (Parkhurst and Appelo, 2013). The measured pH, T, and the K^+, Na^+, Ca^{2+}, Mg^{2+}, HCO_3^-, Cl^-, SO_4^{2-}, and NO_3^- concentrations were used as inputs.

2.5. Statistical approach of the data

The correlations between the nutrient, the ratios of nutrients, and the Chlorophyll *a*, were depicted using SigmaPlot 12.5; the correlations between TN/TP and the relative abundance of Cyanobacteria were also depicted using SigmaPlot 12.5.

3. Results

3.1. Spatio-temporal variations in physiochemical parameters

The physiochemical parameters of the three river-reservoir systems exhibited significant spatial and seasonal variations (Figs. 2 and 3). The T of the river-reservoir systems exhibited significant seasonal variation characterized by the highest temperatures in summer (August 2018) and lowest in winter (January 2019). The T at the river sampling sites ranged from 9.55 °C to 26.52 °C, with an overall mean of 16.42 °C, and that at reservoir sampling sites was 7.4–29.07 °C, with an overall mean of 19.48 °C. The T variation range at PZR and PDR was larger than at the river sampling sites. The pH of the rivers ranged from 7.62 to 8.72 (mean = 8.04), and did not show a clear seasonal variation; however, the pH of the reservoirs ranged from 7.35 to 9.18 (mean = 8.37), and did show higher values during spring-summer and lower during autumn–winter. The pH at reservoir sampling sites also varied a larger range than those at the river sampling sites.

The Ca^{2+} concentrations from the rivers to reservoirs showed clear decreasing trend, especially in PZR and HFR. The highest decrease occurred during the summer, with Ca^{2+} concentrations decreasing from 67.12 mg/L (YCZ) to 25.14 mg/L (PZA) in PZR, and from 53 mg/L (HQQ) to 25.04 mg/L (NH) in HFR. The largest decrease in Ca^{2+} concentrations may be due to the great increase in precipitation of $CaCO_3$ when the BCP effect was the strongest during the summer.

DIC concentrations in the rivers do not exhibit clear seasonal variation patterns, and the variation amplitudes were only 6 mg/L, 12 mg/L, and 7.2 mg/L at sites SCH, LC, and HQQ, respectively (Figs. 2 and 3). By

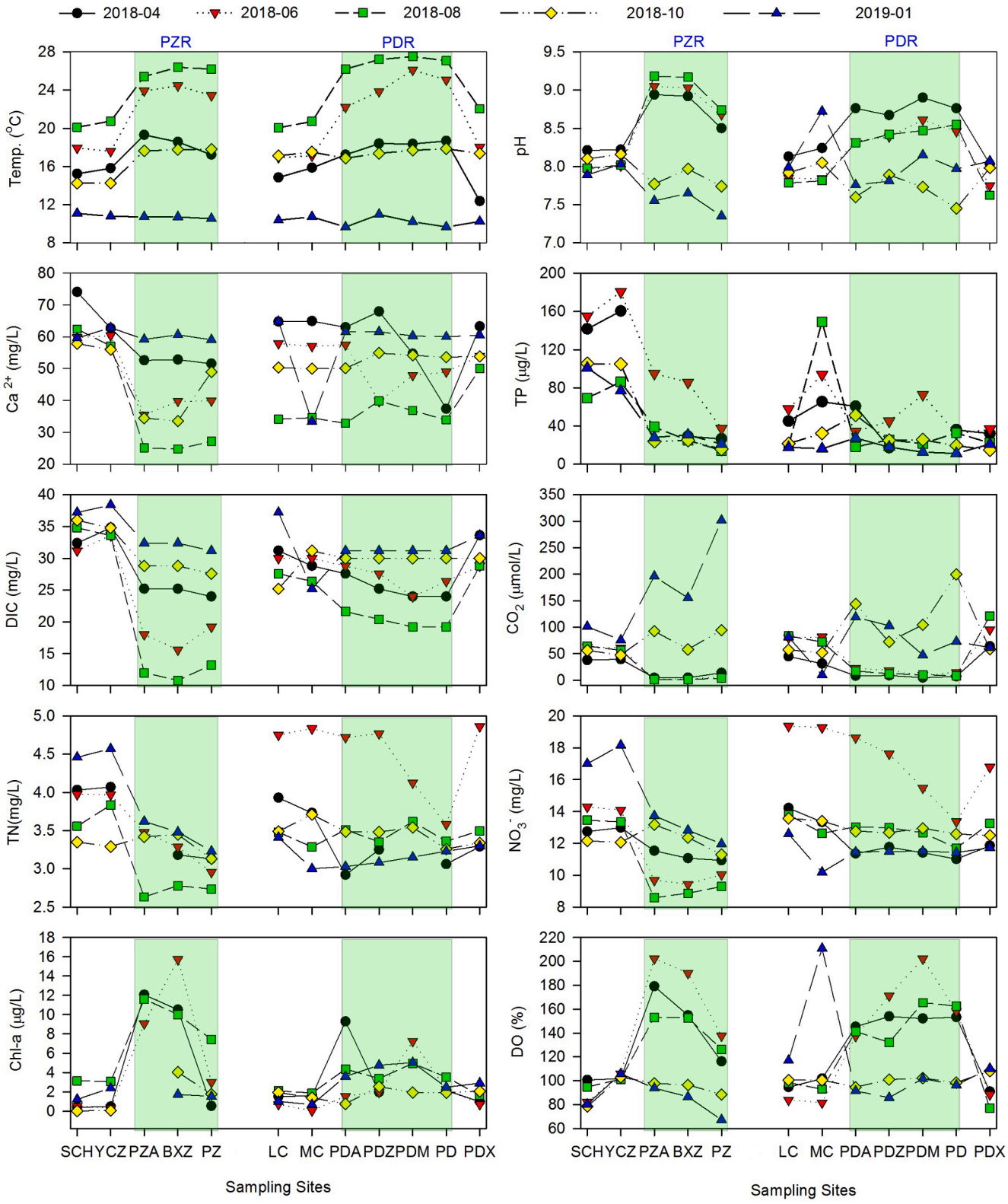

Fig. 2. Seasonal variations in the physiochemical parameters of the Pingzhai (PZR) and Puding river-reservoir (PDR) systems.

contrast, the DIC concentrations in the reservoirs exhibited considerable seasonal patterns, with the highest values in winter (January 2019) and lowest in summer (August 2018), with ranges of 10.8–31.2 mg/L, 19.2–32.4 mg/L, and 14.4–32.4 mg/L for PZR, PDR, and HFR, respectively. The DIC concentrations in the reservoirs were always lower than those in the river. The $CO_{2(aq)}$ concentrations ranged from 9.79 μmol/L to 100.99 μmol/L in river sampling sites, with little variation. By contrast, the $CO_{2(aq)}$ concentrations in the reservoirs ranged from 2.31 μmol/L to 301.7 μmol/L, with significant seasonal patterns (i.e., lower in April, June and August 2018, and higher in October 2018 and January 2019). The largest seasonal variation occurred at PZ with 300.3 μmol/L (4–304.3 μmol/L), which mainly came from the largest $CO_{2(aq)}$

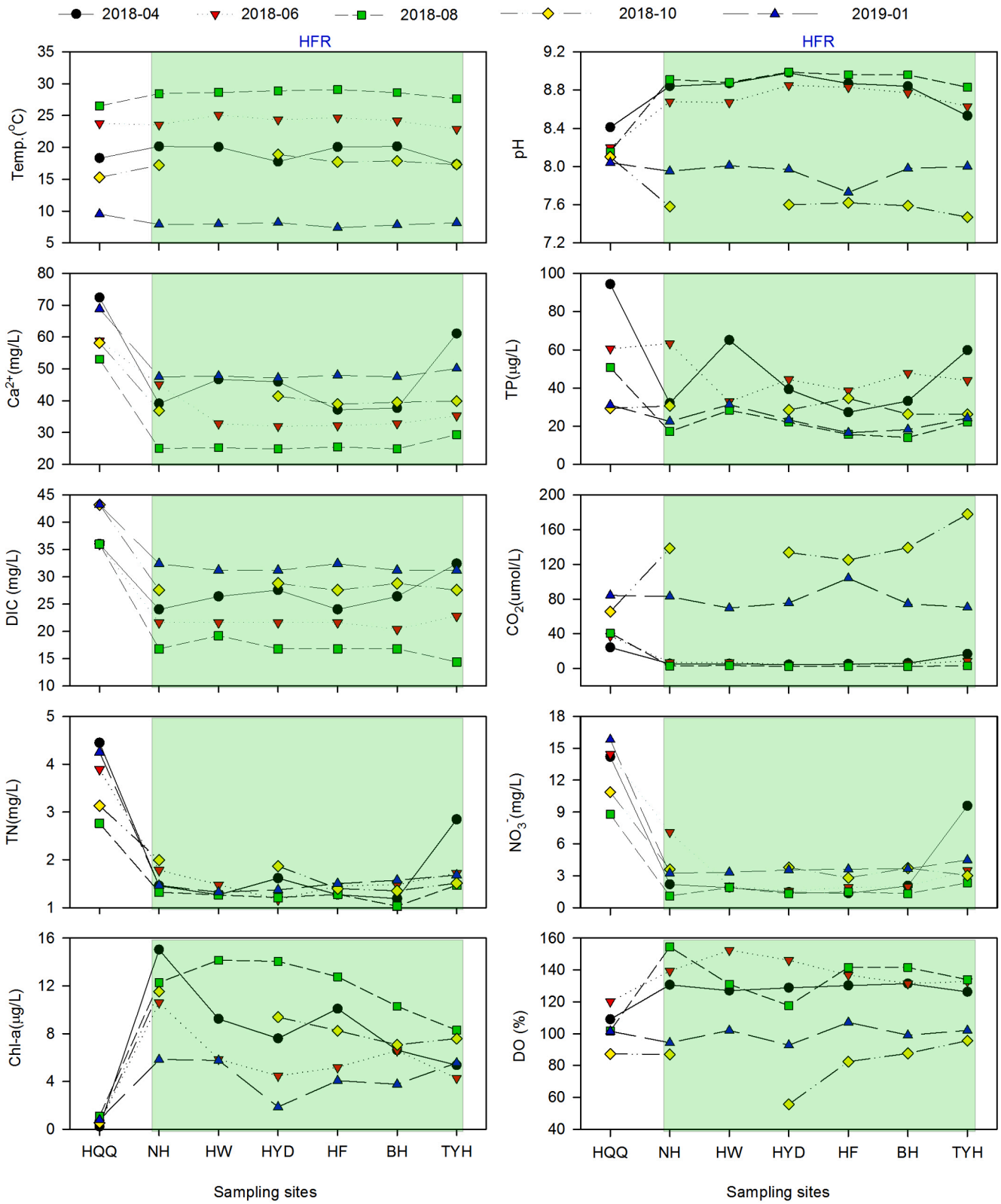

Fig. 3. Seasonal variations in the physiochemical parameters of the Hongfeng river-reservoir (HFR) system.

concentrations in winter due to the decomposition of organic matters.

As shown in Fig. 2, TP concentrations in the Pingzhai river-reservoir system show clear seasonal variations, with the highest values (180.5 μg/L and 94.9 μg/L in the river and reservoir, respectively) in June 2018 and the lowest values (67.8 μg/L and 9.9 μg/L in the river and reservoir, respectively) in August 2018. Similar to the PZR, TP concentrations in the HFR were highest (mean = 42.78 μg/L) in June 2018, and lowest (mean = 19.96 μg/L) in August 2018; and TP concentrations in the river sampling site (HQQ) ranged from 29.32 μg/L to 94.27 μg/L, with the highest and lowest values in April and October 2018, respectively. In the Puding river-reservoir system, TP concentrations had no clear seasonal variations, and ranged from 19.10 μg/L to 149.05 μg/L (mean = 51.79

μg/L).

The TN and NO_3^- concentrations in river sampling sites were 2.76–4.86 mg/L (mean = 3.78 mg/L) and 8.78–19.36 mg/L (mean = 13.76 mg/L), respectively, with no obvius difference between the two rivers. The TN and NO_3^- concentrations in HFR were lower than those in PZR and PDR. The mean concentrations in the HFR (1.49 mg/L and 3.02 mg/L, respectively) were lower than those in the PZR (3.18 mg/L and 10.98 mg/L, respectively) and PDR (3.50 mg/L, and 12.07 mg/L, respectively). In general, TN and NO_3^- were highest in winter (January 2019) and lowest in summer (August 2018) in the Pingzhai and Hongfeng river-reservoir systems. Contrary to that in the PZR and HFR, the TN and NO_3^- concentrations in the Puding river-reservoir system exhibited opposite seasonal variation patterns, with the highest concentrations in summer and lowest in winter.

3.2. Spatio-temporal variations in Chl-a and DO concentrations in the reservoirs

The Chl-*a* and DO concentrations in the Pingzhai river-reservoir and Hongfeng river-reservoir systems exhibited clear seasonal variations, with higher concentrations in summer and lower in winter (Figs. 2 and 3. Within the PZR, the Chl-*a* and DO values ranged from 0.5 to 15.7 μg/L (mean = 6.84 μg/L) and 67.3–202.4% (mean = 129.5%), respectively. Within the HFR, the Chl-*a* concentrations and DO were 1.85–15.0 μg/L (mean = 8.04 μg/L) and 55.6–154.4% (mean = 118.5%), respectively. In the Puding river-reservoir system, the Chl-*a* concentrations in the rivers were relatively stable and exhibited no clear seasonal variations, the mean concentration was 1.40 μg/L. The Chl-*a* concentration in the PDR also showed no obvious seasonal variations and ranged from 0.75 μg/L to 9.29 μg/L (mean = 3.45 μg/L). Contrary to Chl-*a*, the DO concentrations in the PDR exhibited season variations with higher values during spring-summer (April, June, and August 2018) and lower during autumn–winter (October 2018 and January 2019), ranging from 85.7% to 202.1%, with a mean value of 132.3%.

Spatially, the Chl-*a* concentrations were higher in reservoirs and lower in rivers. The DO concentrations were higher in reservoirs than in rivers during spring and winter; conversely, in autumn and winter, the DO concentrations in reservoirs were lower than in rivers.

3.3. Phytoplankton community structure dynamics in the reservoirs

We recorded six phytoplankton groups in PZR and HFR (Fig. 4). The

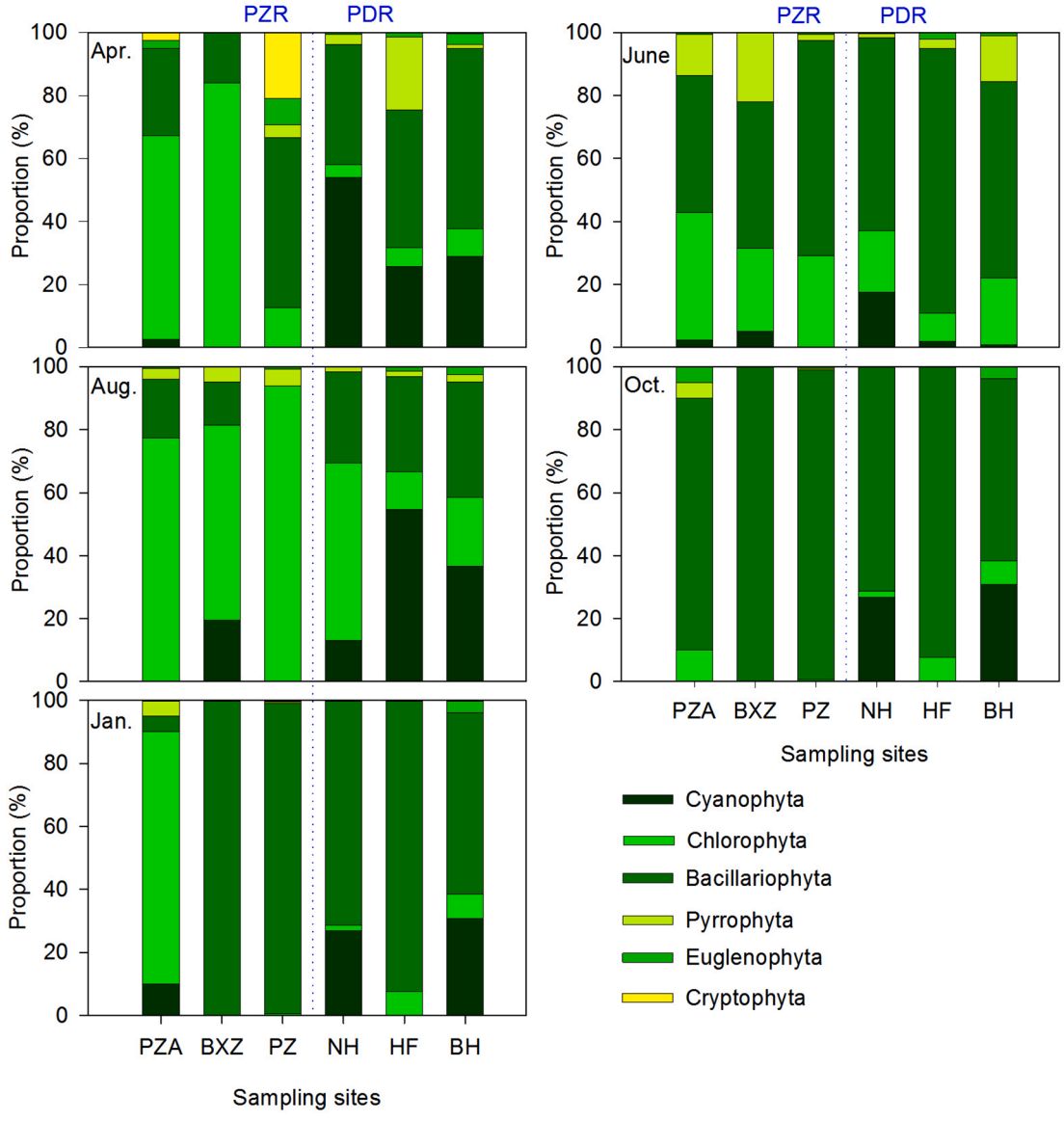

Fig. 4. Variations in the phytoplankton community structure in the PZR and HFR between April 2018 and January 2019.

phytoplankton community structure varied markedly with time and space. In PZR, the dominant groups Bacillariophyta and Chlorophyta, Bacillariophyta appeared mainly in October 2018 and January 2019; Chlorophyta appeared from April to August 2018; Cyanophyta had a relative abundance lower than 20% in PZR. Cyanophyta was not observed at PZ, which was located downstream of PZR. In HFR, the phytoplankton community was dominated by Bacillariophyta in June and October 2018 and January 2019; however, the relative abundance of Cyanophyta (54.54%) was higher than that of Bacillariophyta in August 2018.

3.4. The TP fluxes and phosphorus fractions in settling particulates

Fig. 5a shows the TP fluxes in settling particulates at PZR and HFR, ranging from 1.46 mg/m^2·d to 32.88 mg/m^2·d, and highest at PZR. The mean values of TP flux are 15.29 mg/m^2·d in PZR and 4.88 mg/m^2·d in HFR, respectively. The TP fluxes in seetling particulates show significant spatial variations, which gradually decreased downstream.

Fig. 5b shows the P fractions in settling particulates during June-August 2018. HCl-P is regarded as a Ca-bound P compound which is related to the coprecipitation of P with calcite; BD-P as P associated with Fe hydroxides; and NaOH-SRP as P bound to metal oxides (mainly of Fe and Al) (Kozerski and Kleeberg, 1998). Both of the latter two parts are related to the coprecipitation of P with soild Fe(III) oxyhydroxide. So, we consider that the summation of the proportions of HCl-P, BD-P and NaOH-SRP equals to the mean proportion of P removal by BCPs. The HCl-P, BD-P, and NaOH-SRP ranges are 5.72–41.38% (mean = 15.78%), 11.37–21.43% (mean = 16.35%) and 13.85–41.83% (mean = 33.20%), respectively.

4. Discussion

4.1. Seasonal variations in TN, NO_3^-, and TP concentrations at river sampling sites

Seasonal variations in TN, NO_3^-, and TP concentrations at river sampling sites can be attributed to human activities such as N and P fertilizer application, wastewater disposal, and land-use patterns and practices (Galloway et al., 2008; Carpenter et al., 1998; Vitousek et al.,1997). The variations in NO_3^- concentrations correlate with the variations in TN, which indicates that NO_3^- was the main component of TN in water, and accounted for a mean of 80.3% of TN (Figs. 2 and 3). NO_3^- enters rivers mainly through agricultural runoff (David and Gentry, 2000; Kemp and Dodds, 2001). The seasonal variations in NO_3^- concentrations in midstream of the Sancha River (sites LC, MC, and PDX) were higher in June 2018, which was mainly attributed to fertilizer application and the erosion of agricultural land in the vicinity of the river (Chen et al., 2010; Kemp and Dodds, 2001; Zhang et al., 2020). In contrast, the NO_3^- concentrations in the upper sections of the Sancha River (sites SCH and YCZ) and Yangchang River (site HQQ) were lower in August 2018, which may have contributed to the combined effect of the dilution of rainfall and phytoplankton utilization, which is stronger than the effect of agricultural land erosion (Stelzer et al., 2020; Zhang et al., 2007; Zeng et al., 2019).

The TP concentration in river sampling sites also displayed seasonal variation, and was higher in April and June 2018, mainly due to the application of P fertilizer (Boardman et al, 2019; Heathwaite et al., 2005; Sharpley et al., 2000; Withers and Jarvie, 2008).

4.2. Mechanisms for the seasonal variations in DIC, TN, and NO_3^- concentrations in reservoirs

Seasonal variations in DIC concentration in reservoirs may be controlled by dilution of rainfall, aquatic photosynthesis, and decomposition of organic matter (Liu et al., 2007; Yang et al., 2012; Yang et al., 2015). In reservoirs, the decrease in DIC concentrations in summer may have been attributed to the dilution effect after rainfall (Liu et al., 2007). However, in comparison with that in reservoirs, the minor variation amplitudes of DIC in rivers indicate that the dilution effect is not the key factor controlling the seasonal variations. Thus, the seasonal variations in DIC in reservoirs mainly contribute to the utilization of aquatic photosynthesis (Bao et al., 2020; Müller et al., 2016; Nõges et al. 2016; Yang et al., 2020; Zeng et al., 2019). Here, we used Chl-*a* and DO to characterize aquatic photosynthesis. The lowest DIC values were observed in summer (Aug. 2018), accompanied by the highest Chl-*a* and DO concentrations, demonstrating that the decrease in DIC was mainly caused by phytoplankton utilization (Figs. 2 and 3).

Two seasonal variation patterns were evident in TN and NO_3^- concentrations in reservoirs. TN and NO_3^- concentrations in the surface water of the PDR exhibited strong seasonality, characterized by high concentrations in summer (June 2018) and low in winter (January 2019). The highest TN and NO_3^- concentrations reflect the influence of rivers that introduce large amounts of N to the reservoir (Bode and Dorth, 1996), because N leaches from surface soil to river water by runoff during the rainy season (Chen et al., 2010; Zhang et al., 2020). In the Puding river-reservoir system, croplands are abundant in the vicinity of the river channels and make a disproportionately high contribution to the TN and NO_3^- concentrations in rivers due to their proximity to river channels that are affected by river hydrology (Boardman et al., 2019). In contrast, the PZR and HFR exhibited high concentrations in winter

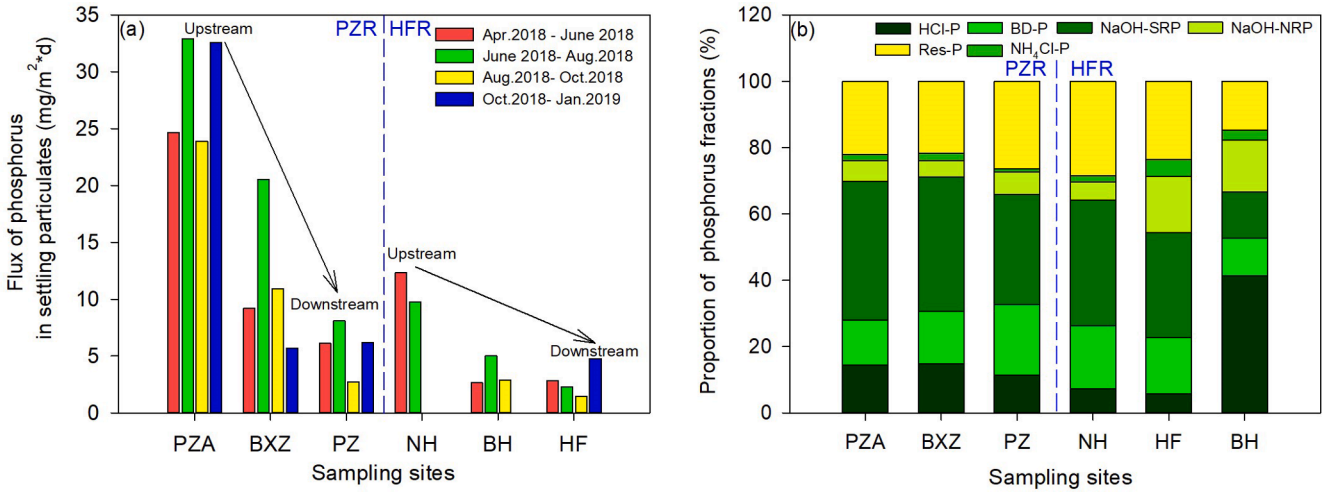

Fig. 5. The flux of total phosphorus (TP) and its chemical fractions in settling particulates.

(January 2019) and low in summer (August 2018). The lowest TN and NO_3^- concentrations in the PZR and HFR may reflect the seasonal variation in N uptake and dilution effect of rainwater that contains lower N concentrations (Stelzer et al., 2020; Zeng et al., 2019; Zhang et al., 2007).

4.3. Spatial variations in TP concentrations in surface water of reservoirs and P removal by the BCP

The TP concentrations in surface water of PZR exhibited significant spatial variations, with gradual decrease along the longitudinal transect from upstream to downstream. For example, the TP concentrations decreased from 94.92 μg/L upstream to 37.36 μg/L downstream in June 2018, and about 60% of the TP is removed from the surface water (Fig. 2). Contrary to the PZR, the TP concentrations in surface water of HFR did not show clear spatial variations (Fig. 3). The largest spatial variation occurred in June 2018 when the TP concentrations decreased from 63.28 μg/L upstream to 38.69 μg/L downstream, and about 40% of the TP removed. Except for June 2018, the spatial variations of TP in HFR were small, not exceeding 6 μg/L.

The gradual decrease of TP concentrations along the longitudinal transect was partly attributable to the P uptake by phytoplankton (Boardman et al., 2019), but mainly the rapid sedimentation of P-containing particulates caused by the P removal by the BCP, which is shown in Fig. 5a (Chen and Liu, 2017; Straškrabová et al., 1994; Walsh et al., 2019). In PZR, the fluxes of P in settling particulates can reach 32.88 $mg/m^2 \cdot d$ with a mean value of 28.51 $mg/m^2 \cdot d$ in the upper section of the river.

The BCPs in karst surface aquatic ecosystems can produce calcite and O (Liu et al., 2018). The calcite promotes the coprecipitation of P in water (Murphy et al., 1983; Otsuki and Wetzel, 1972;), which can also bind to Fe(III) oxyhydroxide colloids and consequently coprecipitate by oxidation of Fe(II) (Gunnars et al., 2002; Hoffman et al., 2013; Hongve, 1997). Moreover, Fe(III) oxyhydroxide colloids can also absorb P from water to form coprecipitates due to the large specific surface area (Chen and Liu, 2017). We considered the HCl-P, BD-P, and NaOH-SRP chemical fractions that were related to BCP. The proportion of three fractions range from 65.92% to 71.12% (mean = 68.96%) in PZR, and 54.35% to 66.60% (mean = 61.72%) in HFR (Fig. 5), implicating that the mean proportions of P removed by BCPs are approximately 68.96% and 61.72% in the PZR and HFR, respectively. Thus, BCPs play an important role in P removal in reservoirs.

4.4. Effect of P removal by BCP on nutrient limitations of phytoplankton primary productivity

Phytoplankton primary productivity and BCPs can be controlled by N, P, or both (Conley et al., 2009; Paerl et al., 2016; Schindler et al., 2008; Smith et al., 2016). In recent years, the C limitation of phytoplankton primary productivity has attracted increasing attention, especially in karst surface waters where the dissolved $CO_{2(ag)}$ may constitute < 1% of the DIC, and HCO_3^- is the dominant component (Bao et al., 2020; Kragh and Sand-Jensen, 2018; Hammer et al., 2019; Zeng et al., 2019). Yang et al. (2016) found that phytoplankton biomass and the DIC concentration were positively correlated in the Pearl River, indicating the DIC fertilization effect on aquatic photosynthesis. Zeng et al. (2019) found that organic C production in the ponds of spring pond systems at a karst test site was limited by C, whereas Bao et al. (2020) found that the phytoplankton density in the ponds of the same system was mainly related to $CO_{2(aq)}$ in January (the dormant period), and NO_3^- and PO_4^{3-} in July (the growth period). In karst cascade reservoirs, Wang et al. (2018) found that water temperature and $CO_{2(aq)}$ and Si concentrations were the controlling factors of algal succession. However, the above studies identified the C limitations of phytoplankton primary productivity through mesocosm studies at karst test sites, or only evaluated the C limitations on algal succession in reservoirs (Bao et al., 2020; Hammer et al., 2019; Wang et al., 2018; Zeng et al., 2019). The BCP effect could also be influenced by other environmental factors (water temperature, light intensity) and hydrodynamic conditions (flow velocity, discharge), espically the highly dynamic discharge conditions in karst regions (Liu et al., 2017; Wang et al.,2018; Yang et al., 2016; Yang et al, 2020). In this study, we focus on the nutrient limitations on primary productivity in karst river-dammed reservoirs under the effect of P removal by BCP.

Ecological stoichiometric ratios have been widely used to study the effects of nutrient limitation on primary productivity in aquatic ecosystems (Elser et al., 2009; Rhee, 1978). In this study, to clarify which element play a key role in phytoplankton primary productivity, stoichiometric C, N, and P ratios (molar ratio) were used. Chl-*a* concentrations were used to represent phytoplankton primary productivity or a BCP.

At the river sampling sites, the DIC/TN, DIC/TP, and TN/TP have positive relationships with Chl-*a*, and the correlation between Chl-*a* and DIC/TP ($R^2 = 0.14$, $P > 0.05$) is higher than that between Chl-*a* and DIC/TN ($R^2 = 0.03$, $P > 0.05$) or TN/TP ($R^2 = 0.12$, $P > 0.05$) (Fig. S1). The resultts indicates that C was the main factor controlling primary productivity in rivers in this study. Our findings are consistent with the result in the Pearl River (Yang et al., 2016) and further confirms that primary productivity in rivers is mainly controlled by C.

Dams impede the flow of essential nutrients, including C, N, and P, leading to increased nutrient retention (Maavara et al., 2020). However, BCP removed the P from the surface water, and probably changed the nutrient limitation pattern from C-limitation to P-limitation. To study the effect of P removal by BCP on nutrient limitations of phytoplankton primary productivity, the relationships of Chl-*a*, nutrients and the stoichiometric ratios of nutrients were researched. In this study, all the reservoirs had clear thermal stratifications in the spring and summer, which gradually disappeared in the autumn and winter. The thermal stratification period corresponds to the phytoplankton growth period, while the mixing period corresponds to the dormant period. Hence, the nutrient limitation of phytoplankton during the growth and dormant periods are discussed separately.

In the PZR and PDR, Chl-*a* shows negative relationships with DIC and NO_3^-, and a positive relationship with TP during the growth period (Fig. 6). The relationship between Chl-*a* and DIC was inversely related to the positive relationship between the river sites in our study, which was also found in the Peal River (Yang et al., 2016). However, we consider these results not contradictory. In rivers, DIC and Chl-*a* showed a positive relationship because the DIC consumed by phytoplankton can be rapidly compensated. However, the rapid consumption of DIC by phytoplankton in reservoirs cannot be promptly balanced, resulting in a decrease in DIC concentration in response to the negative correlation (Wang et al., 2018). The positive relationship between DIC and Chl-*a* in rivers and the negative relationship in reservoirs both demonstrate the C limitation of phytoplankton primary productivity. To better evaluate the nutrient limitations in PZR and PDR, the stoichiometric ratios of C, N, and P were used, and the cross-plots of Chl-*a* with $CO_{2(aq)}/NO_3^-$-N, $CO_{2(aq)}$/TP, and NO_3^--N/TP in the growth and dormant periods are displayed in Fig. 6 and Fig. S2. Fig. 6 shows negative relationships between Chl-*a* and $CO_{2(aq)}/NO_3^-$-N, $CO_{2(aq)}$/TP, and NO_3^--N/TP during the growth period, and the correlations between Chl-*a* and $CO_{2(aq)}$/TP ($R^2 = 0.68$, $P < 0.0001$) were higher than those between Chl-*a* and $CO_{2(aq)}/NO_3^-$-N ($R^2 = 0.66$, $P < 0.0001$) and NO_3^--N/TP ($R^2 = 0.40$, $P < 0.01$) (Fig. 6). The results indicate that TP was the main factor influencing phytoplankton productivity during the growth period, followed by N and C. Inverse to the growth period, Chl-*a* exhibits a positive relationship with NO_3^--N during the dormant period, which indicates that the phytoplankton productivity is limited by N (Fig. S2).

For HFR, Chl-*a* shows a negative relationship with DIC, TN, and TP during the growth period, indicating that phytoplankton productivity is controlled by C, N, and P (Fig. 7). The Chl-*a* also showed positive relationships with DIC/TP and TN/TP, suggesting that the effects of N and C on phytoplankton productivity were greater than that of P (Fig. 8).

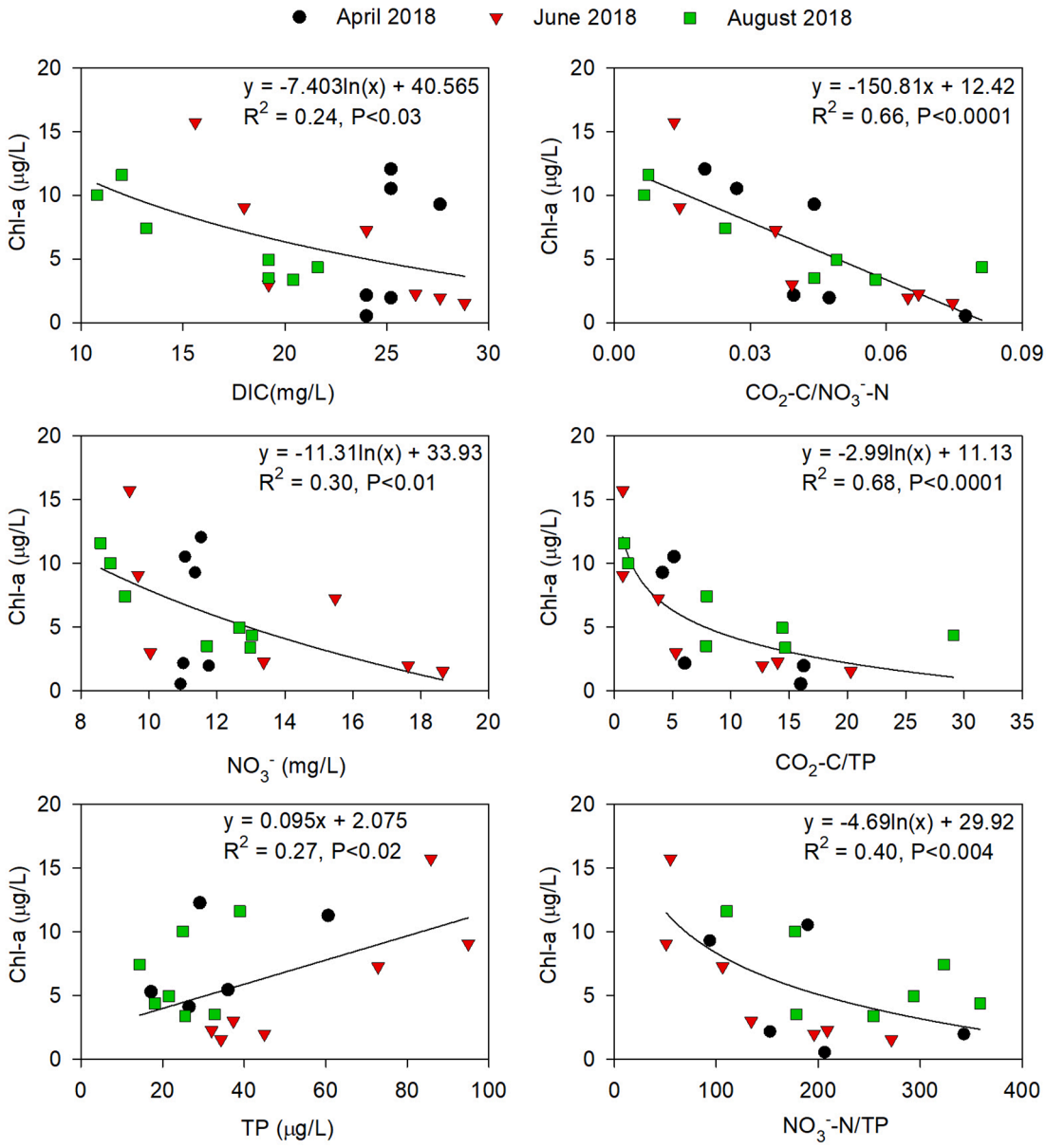

Fig. 6. Relationships between DIC, NO_3^-, TP, $CO_{2(aq)}$ -C/NO_3^--N, $CO_{2(aq)}$ -C/TP, NO_3^--N/TP, and Chl-*a* in the Pingzhai Reservoir (PZR) and Puding Reservoir (PDR) during the growth period.

Combining the negative relationship between Chl-*a* and $CO_{2(aq)}$/TN, the phytoplankton productivity of the HFR during the growth period is mainly controlled by N. In the dormant period, phytoplankton productivity is mainly controlled by P, followed by C and N (Fig. S3).

There were significant differences in nutrient limitation patterns among the PZR, PDR and HFR sites. During the growth period, phytoplankton primary productivity in the PZR and PDR showed significant P-limitation, whereas that in the HFR showed N-limitation. We consider that the P-limitation in the PZR and PDR can be mainly attributed to the P removal by BCP (Chen and Liu, 2017; Straškrabová et al., 1994; Walsh et al., 2019) (Fig. 5). Under the stronger P removal by BCP, TP concentrations in the surface of PZR show a gradual downstream decrease (Figs. 2 and 5), opposite to the TN:TP ratios of downstream increase (Fig. S4). In August 2018, the TN:TP (molar ratio) increases from 149 upstream to 421 (PZA) downstream (PZ) in the PZR. During the growth period, the mean TN:TP ratio reaches 207. Elser et al. (2009) found that phytoplankton were consistently P-limited when TN:TP (molar ratio) was > ~110. Under the effect of P removal by BCP, the phytoplankton primary productivity of PZR shows significant P-limitation (Fig. S4). For the HFR, P removal by BCP is weaker, and the mean flux of TP in sediment traps is 4.88 mg/m^2·d, which is only about one third of the PZR (15.29 mg/m^2·d) (Fig. 5). The decrease of TP in HFR is not obvious, following the non-significant TN:TP ratio downstream increase (Fig. S4). The TN:TP ratio (molar ratio) increases from 100 to 103, 62 to 83, and 170 to 180 in April, June, and August 2018, respectively (Fig. S4). Evidently, P removal by the BCP in the HFR was less efficient than that in the PZR, and the phytoplankton primary productivity of HFR in the growth period exhibited N-limitation.

4.5. *Effect of P removal by BCP and the role in alleviating eutrophication*

Cyanobacteria dominance in eutrophic lakes/reservoirs is a major problem to human and ecosystem health (Downing et al., 2001). Nutrient concentrations control phytoplankton growth, and the stoichiometric ratio of N to P (N:P) can favor Cyanobacteria dominance (Downing et al., 2001; Smith, 1983). Smith (1983) found that Cyanobacteria tended to be rare when the TN/TP (by weight) exceeds 29:1. To evaluate the effect of P removal by BCP on the control of Cyanobacteria

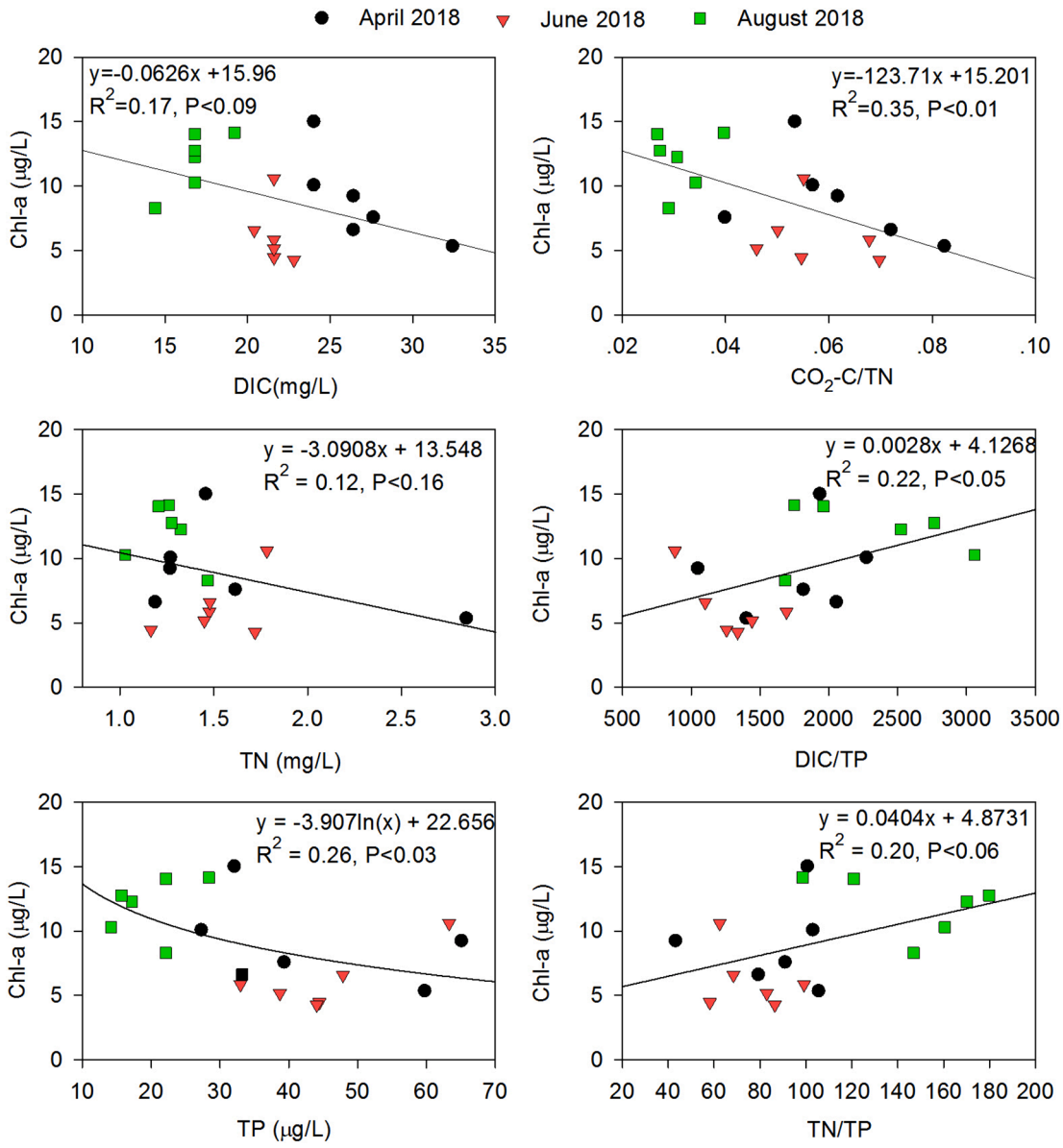

Fig. 7. Relationships between DIC, NO_3^-, TP, $CO_{2(aq)}$ -C/NO_3^--N, $CO_{2(aq)}$ -C/TP, NO_3^--N/TP and Chl-*a* in the Hongfeng Reservoir (HFR) during the growth period.

dominance by nutrient stoichiometry (N:P), we studied the phytoplankton community structure in the PZR and HFR. Fig. 8a shows the spatial–temporal variations in relative abundance of cyanobacteria in PZR and HFR. In PZR, the relative abundance of Cyanobacteria decreases toward the dam due to the increase of TN/TP ratio caused by significant P removal (Fig. S4); moreover, no cyanobacteria were present in the dam site (PZ). In contrast, the relative abundance of Cyanobacteria in HFR are higher, and the relative abundance at the dam site HF is the highest during summer due to the weakened P removal (Fig. 5). Fig. 8b shows a negative relationship between relative abundance of Cyanobacteria and stoichiometric ratios of TN to TP (TN:TP) in the surface water of the HFR and PZR, which indicates that the ratio TN:TP can favor Cyanobacteria dominance in lakes/reservoirs. Fig. 8b also shows that an apparent boundary was evident between a region where Cyanobacteria tends to dominate (TN:TP $<$ 200 by molar) or be rare (TN:TP $>$ 200 by molar). Our results confirm the view that cyanobacteria dominance can be controlled by the stoichiometric ratio of TN to TP (Smith, 1983).

These results demonstrate that P removal by BCPs plays a key role in controlling Cyanobacteria dominance and can alleviate the development of Cyanobacteria-type eutrophication in water bodies.

In karst area, higher concentrations of HCO_3^- and Ca^{2+} due to the rapid kinetics of carbonate mineral dissolution can promote the BCP effect (calcite precipitation and the primary productivity of aquatic phototrophs) (Liu et al., 2011, Yang et al., 2016; Zeng et al., 2019; Bao et al., 2021). Then, the coprecipitation of P with calcite and soild Fe(III) oxyhydroxide which is accelerated by the promoted BCP effect make algal growth in karst waters tends to be strongly P-limited (Hamilton et al., 2009); the increased TN/TP ratio caused by significant P removal change the structure of phytoplankton community through making the relative abundance of Cyanobacteria decreases. As a result of P removal, the proceeding of eutrophication (the primary productivity and the structure of phytoplankton community) is alleviated. In the latest research, Bao et al. (2021) found that the natural restoration of vegetation, or injecting CO_2 into water, which results in higher C but lower N-P loading, may promote the BCP effect. Therefore, the eutrophication in karst area can be alleviated by the promoted BCP effect through the restoration of vegetation, or injecting CO_2 into water, and a win–win status of water quality safety and carbon sink in the water body could be achived.

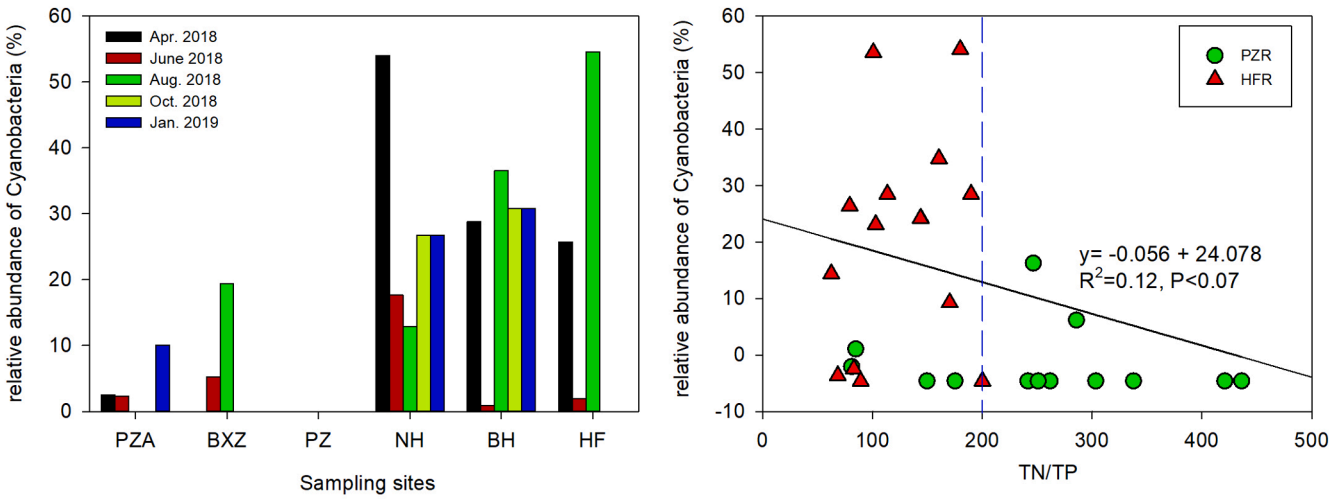

Fig. 8. Spatial-temporal variations in Cyanobacteria relative abundance in the Pingzhai Reservoir (PZR) and Hongfeng Reservoir (HFR) and relation between the relative abundance of Cyanobacteria and stoichiometric ratio of TN:TP.

5. Conclusions

In this study, we documented the spatial–temporal variations in physiochemical parameters and Chl-*a* in dammed karst rivers. BCPs were mainly controlled by C in rivers and by P in the PZR and PDR, and by N in the HFR. By analyzing the TP content of settling particulates in sediment traps, we found a downstream decrease in TP fluxes in the PZR and HFR. The rapid sedimentation of P-containing particulates then caused a gradual decrease in TP concentrations and a gradual increase in the stoichiometric ratio of TN to TP (TN:TP) in the surface water of the PZR and HFR. The fluxes of total P in setting particulates of the PZR were approximately three times larger than those in the HFR. The P-limitation of BCP in the PZR mainly contributed to the decrease in TP concentrations and increase in the stoichiometric ratio of TN to TP (TN:TP) caused by the stronger P removal by BCP. The P fractions revealed that the proportions of P removed by the BCPs were approximately 68.9% and 61.7% in the PZR and HFR, respectively. The increase in the TN:TP ratios in surface water further influenced the phytoplankton community structure in the PZR and HFR. The relative abundance of Cyanobacteria generally showed a downstream decrease due to the increase of TN:TP ratios caused by P removal by the BCP. In particular, no Cyanobacteria were present at the PZR dam. This study demonstrated that nutrient limitation patterns of a BCP shift from C-limitation to N- or P-limitation after the rivers were dammed. Under the effect of P removal, the BCP of PZR was significantly P-limited. Phosphorus removal by BCPs can be used to evaluate the development of eutrophication by decreasing the relative abundance of Cyanobacteria. This study may have important implications for the eutrophication control in HCO_3-Ca type surface waters, especially in karst areas, which cover about 15% of the world land surface. In karst water bodies (rivers, lakes and reservoirs), high concentrations of Ca^{2+} and HCO_3^- due to the rapid kinetics of carbonate mineral dissolution may promote calcite precipitation, then promote the coprecipitation of P with calcite; the high concentrations of DIC may also promote the primay productivity and increase the pH and DO concentrations of the karst waters which promote the the coprecipitation of P with Fe(III) oxyhydroxide colloids. It is predicted that the proceeding of eutrophication in HCO_3-Ca type surface waters (lakes/reservoirs), with Ca^{2+} the major cation, and HCO_3^- the major anion, may be retarded through regulating the phytoplankton productivity and the relative abundance of Cyanobacteria caused by the P limitation and relatively higher TN:TP ratios deriving by P removal by BCPs.

Declaration of Competing Interest

The authors declare that they have no known competing financial interests or personal relationships that could have appeared to influence the work reported in this paper.

Acknowledgments

This study was financially supported by the National Natural Science Foundation of China (42130501, 42141008, U1612441, 41977298, and 41921004), the Strategic Priority Research Program of the Chinese Academy of Sciences (XDB40020000) and the Key Research and Development Program of Guangxi Zhuang Autonomous Region, China (AB21196050).

Appendix A. Supplementary data

Supplementary data to this article can be found online at https://doi.org/10.1016/j.jhydrol.2022.127480.

References

Abell, J.M., Özkundakci, D., Hamilton, D.P., 2010. Nitrogen and phosphorus limitation of phytoplankton growth in New Zealand lakes: Implications for eutrophication control. Ecosystems 13 (7), 966–977. https://doi.org/10.1007/s10021-010-9367-9.

Andersen, M.R., Kragh, T., Martinsen, K.T., Kristensen, E., Sand-Jensen, K., 2019. The carbon pump supports high primary production in a shallow lake. Aquat. Sci. 81, 24. https://doi.org/10.1007/s00027-019-0622-7.

Bao, Q., Liu, Z., Zhao, M., Hu, Y., Li, D., Han, C., Wei, Y.u., Ma, S., Zhang, Y.i., 2020. Primary productivity and seasonal dynamics of planktonic algae species composition in karst surface waters under different land uses. J. Hydrol. 591, 125295. https://doi.org/10.1016/j.jhydrol.2020.125295.

Bao, Q., Liu, Z., Zhao, M., Hu, Y., Li, D., Han, C., Zeng, C., Chen, B.o., Wei, Y.u., Ma, S., Wu, Y., Zhang, Y.i., 2021. Role of carbon and nutrient exports from different land uses in the aquatic carbon sequestration and eutrophication process. Sci. Total Environ. 151917. https://doi.org/10.1016/j.scitotenv.2021.151917.

Boardman, E., Danesh-Yazdi, M., Foufoula-Georgiou, E., Dolph, C.L., Finlay, J.C., 2019. Fertilizer, landscape features and climate regulate phosphorus retention and river export in diverse Midwestern watersheds. Biogeochemistry 146 (3), 293–309. https://doi.org/10.1007/s10533-019-00623-z.

Bode, A., Dorth, Q., 1996. Uptake and regeneration of inorganic nitrogen in coastal waters influenced by the Mississippi river spatial and seasonal variations. J. Plankton Res. 18 (12), 2251–2268. https://doi.org/10.1093/plankt/18.12.2251.

Carpenter, S.R., Caraco, N.F., Correll, D.L., Howarth, R.W., Sharpley, A.N., Smith, V.H., 1998. Nonpoint pollution of surface waters with phosphorus and nitrogen. Ecol. Appl. 8 (3), 559–568. https://doi.org/10.1890/1051-0761(1998)008[0559:NPOSWW]2.0.CO;2.

Chen, B., Yang, R., Liu Z., Sun, H., Yan, H., Zeng, Q., Zeng, S., Zeng, C., 2017. Coupled control of land uses and aquatic biological processes on the diurnal hydrochemical variations in five ponds at the Shawan Karst Test Site: implications for the carbonate

weathering-related carbon sink. Chem. Geol. 456, 58–71. https://doi.org/ 10.1016/j.chemgeo.2017.03.006.
CHEN, ChongYing, LIU, ZaiHua, 2017. The role of biological carbon pump in the carbon sink and water environment improvement in karst surface aquatic ecosystems (in Chinese). Chin. Sci. Bull. 62 (30), 3440–3450. https://doi.org/10.1360/N972017-00298.
Chen, J., Yu, J., Bai, X., Zeng, Y., Wang, J., 2020. Fragility of karst ecosystem and environment: Long-term evidence from lake sediments. Agr. Ecosyst. Environ. 294, 106862. https://doi.org/10.1016/j.agee.2020.106862.
Chen, X., Wo, F., Chen, C., Fang, K., 2010. Seasonal changes in the concentrations of nitrogen and phosphorus in farmland drainage and groundwater of the Taihu Lake region of China. Environ. Monit. Assess. 169 (1-4), 159–168. https://doi.org/10.1007/s10661-009-1159-3.
Conley, D.J., Paerl, H.W., Howarth, R.W., Boesch, D.F., Seitzinger, S.P., Havens, K.E., Lancelot, C., Likens, G.E., 2009. Controlling Eutrophication: Nitrogen and Phosphorus. Science 323 (5917), 1014–1015. https://doi.org/10.1126/science.1167755.
Corman, J.R., Moody, E.K., Elser, J.J., 2015. Stoichiometric impact of calcium carbonate deposition on nitrogen and phosphorus supplies in three montane streams. Biogeochemistry 126 (3), 285–300. https://doi.org/10.1007/s10533-015-0156-6.
Corman, J.R., Moody, E.K., Elser, J.J., 2016. Calcium carbonate deposition drives nutrient cycling in a calcareous headwater stream. Ecol. Monogr. 86 (4), 448–461. https://doi.org/10.1002/ecm.1229.
Correll, D.L., 1998. The role of phosphorus in the eutrophication of receiving waters: A review. J. Environ. Qual. 27 (2), 261–266. https://doi.org/10.2134/jeq1998.00472425002700020004x.
David, M.B., Gentry, L.E., 2000. Anthropogenic inputs of nitrogen and phosphorus and riverine export for Illinois. USA. J. Environ. Qual. 29 (2), 494–508. https://doi.org/10.2134/jeq2000.00472425002900020018x.
Downing, J.A., Watson, S.B., McCauley, E., 2001. Predicting cyanobacteria dominance in lakes. Can. J. Fish. Aquat. Sci. 58 (10), 1905–1908. https://doi.org/10.1139/f01-143.
Elser, J.J., Andersen, T., Baron, J.S., Bergström, A., Jansson, M., Kyle, M., Nydick, K.R., Steger, L.S., Hessen, D.O., 2009. Shift in lake N: P Stoichiometry and nutrient limitation driven by atmospheric nitrogen deposition. Science 326, 835–837. https://doi.org/10.1126/science.1176199.
Galloway, J.N., Townsend, A.R., Erisman, J.W., Bekunda, M., Cai, Z., Freney, J.R., Martinelli, L.A., Seitzinger, S.P., Sutton, M.A., 2008. Transformation of the Nitrogen Cycle: Recent Trends, Questions, and Potential Solutions. Science 320 (5878), 889–892. https://doi.org/10.1126/science.1136674.
Gao, J., Wang, H., 2019. Temporal analysis on quantitative attribution of karst soil erosion: A case study of a peak-cluster depression basin in Southwest China. Catena 172, 369–377. https://doi.org/10.1016/j.catena.2018.08.035.
Gunnars, A., Blomqvist, S., Johansson, P., Andersson, C., 2002. Formation of Fe (III) oxyhydroxide colloids in freshwater and brackish seawater, with incorporation of phosphate and calcium. Geochem. Cosmochim. Acta 66 (5), 745–758. https://doi.org /10.1016/ S0016-7037(01)00818-3.
Hamdan, M., Byström. P., Hotchkiss, E.R., Al-Haidarey, M.J., Ask, J., Karlsson, J., 2018. Carbon dioxide stimulates lake primary production. Sci. Rep. 8, 10878. https://doi.org/10.1038/s41598-018-29166-3.
Hamilton, S.K., Bruesewitz, D.A., Horst, G.P., Weed, D.B., Sarnelle, O., 2009. Biogenic calcite–phosphorus precipitation as a negative feedback to lake eutrophication. Can. J. Fish. Aquat. Sci. 66, 343–350. https://doi.org/10.1139/F09-003.
Hammer, K.J., Kragh, T., Sand-Jensen, K., 2019. Inorganic carbon promotes photosynthesis, growth, and maximum biomass of phytoplankton in eutrophic water bodies. Freshwater Biol. 64 (11), 1956–1970. https://doi.org/10.1111/fwb.v64.1110.1111/fwb.13385.
He, H., Liu, Z., Chen, C., Wei, Y.u., Bao, Q., Sun, H., Yan, H., 2020. The sensitivity of the carbon sink by coupled carbonate weathering to climate and land-use changes: Sediment records of the biological carbon pump effect in Fuxian Lake, Yunnan, China, during the past century. Sci. Total Environ. 720, 137539. https://doi.org/10.1016/j.scitotenv.2020.137539.
Heathwaite, A.L., Dils, R.M., Liu, S., Carvalho, L., Brazier, R.E., Pope, L., Hughes, M., Phillips, G., May, L., 2005. A tiered risk-based approach for predicting diffuse and point source phosphorus losses in agricultural areas. Sci. Total Environ. 344 (1–3), 225–239. https://doi.org/10.1016/j.scitotenv.2005.02.034.
HEIN, METTE, 1997. Inorganic carbon limitation of photosynthesis in lake phytoplankton. Freshwater Biol. 37 (3), 545–552. https://doi.org/10.1046/j.1365-2427.1997.00180.x.
Hein, M., Sand-Jensen, K., 1997. CO_2 increases oceanic primary production. Nature 388 (6642), 526–527. https://doi.org/10.1038/41457.
Hoffman, A.R., Armstrong, D.E., Lathrop, R.C., Prairie, Y., 2013. Influence of phosphorus scavenging by iron in contrasting dimictic lakes. Can. J. Fish. Aqua. Sci. 70 (7), 941–952. https://doi.org/10.1139/cjfas-2012-0391.
Hongve, D., 1997. Cycling of iron, manganese, and phosphate in a meromictic lake. Limnol. Oceanogr. 42 (4), 635–647. https://doi.org/10.4319/lo.1997.42.4.0635.
Hou, W., Gao, J., 2019. Simulating runoff generation and its spatial correlation with environmental factors in Sancha River Basin: The southern source of the Wujiang River. J. Geogr. Sci. 29 (3), 432–448. https://doi.org/10.1007/s11442-019-1608-z.
Humborg, C., Ittekkot, V., Cociasu, A., Bodungen, B., 1997. Effect of Danube River dam on Black Sea biogeochemistry and ecosystem structure. Nature 386 (6623), 385–388. https://doi.org/10.1038/386385a0.
Hupfer, M., Gächter, R., Ruegger, A., 1995. Poly-P in lake sediments: ^{31}P-NMR spectroscopy as a tool for its identification. Limnol. Oceanogr. 40, 610–617. https://doi.org/10.4319/lo.1995.40.3.0610.
Jensen, H.S., Thamdrup, B.o., 1993. Iron-bound phosphorus in marine sediments as measured by bicarbonate-dithionite extraction. Hydrobiologia 253 (1-3), 47–59. https://doi.org/10.1007/BF00050721.
Kemp, M.J., W. K. Dodds. 2001. Spatial and temporal patterns of nitrogen in pristine and agriculturally influenced streams. Biogeochemistry 53, 125–141. 10.1023/ A: 1010707632340.
Kleiner, J., 1988. Coprecipitation of phosphate with calcite in lake water: a laboratory experiment modeling phosphorus removal with calcite in Lake Constance. Water Res. 22, 1259–1265.://doi.org/10.1016/0043-1354(88)90113-3.
Kozerski, H.P., Kleeberg, A., 1998. The Sediments and Benthic-Pelagic Exchange in the Shallow Lake Mtiggelsee (Berlin, Germany). Internat. Rev. Hydrobiol. 83 (1), 77–112. https://doi.org/10.1002/iroh.19980830109.
Kragh, T., Sand-Jensen, K., 2018. Carbon limitation of lake productivity. Proc. R. Soc. B. 285, 20181415. https://doi.org/10.1002/iroh.19980830109.
Liu, Z., Li, Q., Sun, H., Liao, C., Li, H., Wang, J., Wu, K., 2006. Diurnal variations of hydrochemistry in a travertine-depositing stream at Baishuitai, Yunnan. SW China. Aqua. Geochem. 12 (2), 103–121. https://doi.org/10.1007/s10498-005-2962-2.
Liu, Z., Li, Q., Sun, H., Wang, J., 2007. Seasonal, diurnal and storm–scale hydrochemical variations of typical epikarst springs in subtropical karst areas of SW China: Soil CO_2 and dilution effects. J. Hydrol. 337, 207–223. https://doi.org/10.1016/j.jhydrol.2007.01.034.
Liu, Z., Dreybrodt, W., Wang, H., 2010. A new direction in effective accounting for the atmospheric CO_2 budget: Considering the combined action of carbonate dissolution, the global water cycle and photosynthetic uptake of DIC by aquatic organisms. Earth-Sci. Rev. 99 (3-4), 162–172. https://doi.org/10.1016/j.earscirev.2010.03.001.
Liu, Z., Dreybrodt, W., Liu, H., 2011. Atmospheric CO_2 sink: silicate weathering or carbonate weathering? Appl. Geochem. 26, 292–294. https://doi.org/10.1016/j.apgeochem.2011.03.085.
Liu, H., Liu, Z., Macpherson, G.L., Yang, R., Chen, B., Sun, H., 2015. Diurnal hydrochemical variations in a karst spring and two ponds, Maolan Karst experimental Site, China: biological pump effects. J. Hydrol. 522, 407–417. https://doi.org/10.1016/j.jhydrol.2015.01.011.
Liu, Z., Zhao, M., Sun, H., Yang, R., Chen, B., Yang, M., Zeng, Q., Zeng, H., 2017. “old” carbon entering the south china sea from the carbonate-rich pearl river basin: coupled action of carbonate weathering and aquatic photosynthesis. Appl. Geochem. 78, 96-104. 10.1016/j.apgeochem.2016.12.014.
Liu, Z., Macpherson, G.L., Groves, G., Martin, J.B., Yuan, D., Zeng, S., 2018. Large and active CO_2 uptake by coupled carbonate weathering. Earth-Sci. Rev. 182, 42–49. https://doi.org/10.1016/j.earscirev.2010.03.001.
Maavara, T., Dürr, H.H., Cappellen, P.V., 2014. Worldwide retention of nutrient silicon by river damming: From sparse data set to global estimate. Global Biogeochem. Cy. 28 (8), 842–855. https://doi.org/10.1002/2014GB004875.
Maavara, T., Parsons, C.T., Ridenour, C., Stojanovic, S., Dürr, H.H., Powley, H.R., Van Cappellen, P., 2015. Global phosphorus retention by river damming. Proc. Natl. Acad. Sci. 112 (51), 15603–15608. https://doi.org/10.1073/pnas.1511797112.
Maavara, T., Chen, Q., Van Meter, K., Brown, L.E., Zhang, J., Ni, J., Zarfl, C., 2020. River dam impacts on biogeochemical cycling. Nat. Rev. Earth Environ. 1 (2), 103–116. https://doi.org/10.1038/s43017-019-0019-0.
Mayer, L.M., Liotta, F.P., Norton, S.A., 1982. Hypolimnetic redox and phosphorus cycling in hypereutrophic Lake Sebasticook. Maine. Water Res. 16 (7), 1189–1196. https://doi.org/10.1016/0043-1354(82)90137-3.
Murphy, T.P., Hall, K.J., Yesaki, I., 1983. Coprecipitation of phosphate with calcite in a naturally eutrophic lake. Limnol. Oceanogr. 28 (1), 58–69. https://doi.org/10.4319/lo.1983.28.1.0058.
Müller, B., Meye, J.S., Gächter, R., 2016. Alkalinity regulation in calcium carbonate-buffered lakes. Limnol. Oceanogr. 61 (1), 341–352. https://doi.org/10.1002/lno.10213.
Nõges, P., Cremona, F., Laas, A., Martma, T., Rõõm, E.-I., Toming, K., Viik, M., Vilbaste, S., Nõges, T., 2016. Role of a productive lake in carbon sequestration within a calcareous catchment. Sci. Total Environ. 550, 225–230.
Otsuki, A., Wetzel, R.G., 1972. Coprecipitation of phosphate with carbonates in a marl lake. Limnol. Oceanogr. 17 (5), 763–767. https://doi.org/10.4319/lo.1972.17.5.0763.
Paerl, H.W., Xu, H., McCarthy, M.J., Zhu, G., Qin, B., Li, Y., Gardner, W.S., 2011. Controlling harmful cyanobacterial blooms in a hyper-eutrophic lake (Lake Taihu, China): The need for a dual nutrient (N & P) management strategy. Water Res 45, 1973–1983. https://doi.org/10.1016/j.watres.2010.09.018.
Paerl, H.W., Scott, J.T., McCarthy, M.J., Newell, S.E., Gardner, W.S., Havens, K.E., Hoffman, D.K., Wilhelm, S.W., Wurtsbaugh, W.A., 2016. It takes two to tango: when and where dual nutrient (N & P) reductions are needed to protect lakes and downstream ecosystems. Environ. Sci. Technol. 50 (20), 10805–10813.
Pápista, É., Ács, É., Böddi, B., 2002. Chlorophyll-a determination with ethanol – a critical test. Hydrobiologia 485, 191–198. https://doi.org/10.1023/A:1021329602685.
Parkhurst, D.L., Appelo, C.A.J., 2013. PHREEQC (Version 3) –A computer program for speciation, batchreaction, one-dimensional transport, and inverse geochemical calculations. In: Chapter 43 of Section A: Groundwater in Book 6 Modeling Techniques. https://doi.org/10.3133/tm6A43.
Rhee, G.Y., 1978. Effects of N: P atomic ratios and nitrate limitation on algal growth, cell composition, and nitrate uptake. Limnol. Oceanogr. 23 (1), 10–25. https://doi.org/10.4319/lo.1978.23.1.0010.
Riebesell, U., Wolf-Gladrow, D.A., Smetacek, V., 1993. Carbon dioxide limitation of marine phytoplankton growth rates. Nature 361 (6409), 249–251. https://doi.org/10.1038/361249a0.
Ruban, V., López-Sánchez, J.F., Pardo, P., Rauret, G., Muntau, H., Quevauviller, P., 2001. Development of a harmonised phosphorus extraction procedure and certification of a

sediment reference material. J. Environ Monit. 3, 121–125. https://doi.org/10.1039/B005672N.
Schindler, D.W., 1974. Eutrophication and recovery in experimental lakes: implications for lake management. Science 184 (4139), 897–899.
Schindler, D.W., 1977. Evolution of phosphorus limitation in lakes: Natural mechanisms compensate for deficiencies of nitrogen and carbon in eutrophied lakes. Science 195 (4275), 260–262. https://doi.org/10.1126/science.195.4275.260.
Schindler, D.W., Hecky, R.E., Findlay, D.L., Stainton, M.P., Parker, B.R., Paterson, M., Beaty, K.G., Lyng, M., Kasian, S.E.M., 2008. Eutrophication of lakes cannot be controlled by reducing nitrogen input: Results of a 37 year whole ecosystem experiment. Proc. Natl. Acad. Sci. 105 (32), 11254–11258. https://doi.org/10.1073/pnas.0805108105.
Schindler, D.W., Carpenter, S.R., Chapra, S.C., Hecky, R.E., Orihel, D.M., 2016. Reducing phosphorus to curb lake eutrophication is a success. Environ. Sci. Technol. 50 (17), 8923–8929. https://doi.org/10.1021/acs.est.6b02204.
Schulte, P., van Geldern, R., Freitag, H., Karim, A., Négrel, P., Petelet-Giraud, E., Probst, A., Probst, J.-L., Telmer, K., Veizer, J., Barth, J.A.C., 2011. Applications of stable water and carbon isotopes in watershed research: weathering, carbon cycling, and water balances. Earth-Sci. Rev. 109 (1-2), 20–31. https://doi.org/10.1016/j.earscirev.2011.07.003.
Sharpley, A.N., Foy, B., Withers, P., 2000. Practical and innovative measures for the control of agricultural phosphorus to water: an overview. J. Environ Qual. 29 (1), 1–9. https://doi.org/10.2134/jeq2000.00472425002900010001x.
Smith, V.H., 1983. Low nitrogen to phosphorus ratios favor dominance by blue-green-algae in lake phytoplankton. Science 221 (4611), 669–671.
Smith, V.H., 2003. Eutrophication of freshwater and coastal marine ecosystems: A global problem. Environ. Sci. Pollut. Res. 10 (2), 126–139. https://doi.org/10.1065/espr2002.12.142.
Smith, V.H., Wood, S.A., McBride, C.G., David, J.A., Hamilton, P., Abell, J., 2016. Phosphorus and nitrogen loading restraints are essential for successful eutrophication control of Lake Rotorua. New Zealand, Inland Waters 6 (2), 273–283. https://doi.org/10.5268/IW-6.2.998.
Stauffer, R.E., Armstrong, D.E., 1986. Cycling of iron, manganese, silica, phosphorus, calcium, and potassium in two stratified basins of Shagawa Lake. Minnesota. Geochim. Cosmochim. Acta 50, 215–229. https://doi.org/10.1016/0016-7037(86)90171-7.
Stelzer, R.S., Parr, T.B., Coulibaly, M., 2020. A ten year record of nitrate retention and solute trends in a Wisconsin sand plains stream: temporal variation at multiple scales. Biogeochemistry 147 (2), 125–147. https://doi.org/10.1007/s10533-019-00631-z.
Sterner, R.W., 2008. On the phosphorus limitation paradigm for lakes. Int. Rev. Hydrobiol. 93 (4-5), 433–445. https://doi.org/10.1002/iroh.v93:4/510.1002/iroh.200811068.
Straškrabová, V., Hejzlar, J., Procházková, L., Vyhnálek, V., 1994. Eutrophication in stratified deep reservoirs. Wat. Sci. Tech 30 (10), 273–279. https://doi.org/10.2166/wst.1994.0537.
Stumm, W., Morgan, J., 1981. Aquatic chemistry: an introduction emphasizing chemical equilibria in natural waters. John Wiley & Sons.
Tang, Q.H., Peng, L., Yang, Y., Lin, Q.Q., Qian, S.S., Han, B.P., 2019. Total phosphorus precipitation and chlorophyll a-phosphorus relationships of lakes and reservoirs mediated by soil iron at regional scale. Water Res. 154, 136–143. https://doi.org/10.1016/j.watres.2019.01.038.
Van Cappellen, P., Maavara, T., 2016. Rivers in the Anthropocene: Global scale modifications of riverine nutrient fluxes by damming. Ecohydrol. Hydrobiol. 16 (2), 106–111. https://doi.org/10.1016/j.ecohyd.2016.04.001.
Van Dam, B.R., Tobias, C., Holbach, A., Paerl, H.W., Zhu, G., 2018. CO_2 limited conditions favor cyanobacteria in a hypereutrophic lake: An empirical and theoretical stable isotope study. Limnol. Oceanogr. 63 (4), 1643–1659. https://doi.org/10.1002/lno.v63.410.1002/lno.10798.
Verspagen, J.M.H., Van de Waal, D.B., Finke, J.F., Visser, P.M., Van Donk, E., Huisman, J., 2014. Rising CO_2 levels sill intensify phytoplankton blooms in eutrophic and hypertrophic lakes. PLoS One 9, e104325. https://doi.org/10.1371/journal.pone.0104325.
Vitousek, P.M., Aber, J.D., Howarth, R.W., Likens, G.E., Matson, P.A., Schindler, D.W., Schlesinger, W.H., Tilman, D.G., 1997. Human alteration of the global nitrogen cycle: Causes and consequences. Ecol. Appl. 7 (3), 737–750. https://doi.org/10.2307/2269431.
Wang, B., Qiu, X.L., Peng, X., Wang, F., 2018. Phytoplankton community structure and succession in karst cascade reservoirs. SW China. Inland Waters 8 (2), 229–238. https://doi.org/10.1080/20442041.2018.1443550.
Wang, H.J., Wang, H.Z., 2009. Mitigation of lake eutrophication: loosen nitrogen control and focus on phosphorus abatement. Prog. Nat. Sci. 19 (10), 1445–1151. 10.1016/j.pnsc.2009.03.009.
Wang, W., Li, S.-L., Zhong, J., Li, C., Yi, Y., Chen, S., Ren, Y., 2019. Understanding transport and transformation of dissolved inorganic carbon (DIC) in the reservoir system using $\delta^{13}C_{DIC}$ and water chemistry. J. Hydrol. 574, 193–201. https://doi.org/10.1016/j.jhydrol.2019.04.036.
Walsh, J.R., Corman, J.R., Munoz, S.E., 2019. Coupled long-term limnological data and sedimentary records reveal new control on water quality in a eutrophic lake. Limnol. Oceanogr. 64, S34–S48. https://doi.org/10.1002/lno.11083.
Withers, P.J.A., Jarvie, H.P., 2008. Delivery and cycling of phosphorus in rivers: a review. Sci. Total Environ. 400 (1-3), 379–395. https://doi.org/10.1016/j.scitotenv.2008.08.002.
Wu, B., Wang, G., Wang, Z., Liu, C., Ma, J., 2017. Integrated hydrologic and hydrodynamic modeling to assess water exchange in a data-scarce reservoir. J. Hydrol. 555, 15–30. https://doi.org/10.1016/j.jhydrol.2017.09.057.
Yang, M., Liu, Z., Sun, H., Yang, R., Chen, B.o., 2016. Organic carbon source tracing and DIC fertilization effect in the Pearl River: insights from lipid biomarker and geochemical analysis. Appl. Geochem. 73, 132–141.
Yang, R., Liu, Z., Zeng, C., Zhao, M., 2012. Response of epikarst hydrochemical changes to soil CO_2 and weather conditions at Chenqi, Puding, SW China. J. Hydrol. 468–469, 151–158. https://doi.org/10.1016/j.jhydrol.2012.08.029.
Yang, R., Chen, B., Liu, H., Liu, Z., Yan, H., 2015. Carbon sequestration and decreased CO_2 emission caused by terrestrial aquatic photosynthesis: insights from diel hydrochemical variations in an epikarst spring and two spring-fed ponds in different seasons. Appl. Geochem. 63, 248–260. https://doi.org/10.1016/j.apgeochem.2015.09.009.
Yang, R., Sun, H., Chen, B.o., Yang, M., Zeng, Q., Zeng, C., Huang, J., Luo, H., Lin, D., 2020. Temporal variations in riverine hydrochemistry and estimation of the carbon sink produced by coupled carbonate weathering with aquatic photosynthesis on land: an example from the Xijiang River, a large subtropical karst-dominated river in China. Environ. Sci. Pollut. Res. 27 (12), 13142–13154. https://doi.org/10.1007/s11356-020-07872-8.
Yuan, H., Tai, Z., Li, Q., Liu, E., 2020. In-situ, high-resolution evidence from watersediment interface for significant role of iron bound phosphorus in eutrophic lake. Sci. Total Environ. 706, 136040. https://doi.org/10.1016/j.scitotenv.2019.136040.
Zeng, S., Liu, H., Chen, B., Liu, Z., Zeng, C., Zhao, M., Sun, H., Zeng, Q., Yang, R., Yang, M., Hu, Y., 2019. Seasonal and diurnal variations in DIC, NO_3^- and TOC concentrations of spring-pond ecosystems under different land-uses at Shawan Karst Test Site, SW China: Carbon limitation of aquatic photosynthesis. J. Hydrol. 574, 811–821. https://doi.org/10.1016/j.jhydrol.2019.04.090.
Zhang, J., Liu, S.M., Ren, J.L., Wu, Y., Zhang, G.L., 2007. Nutrient gradients from the eutrophic Changjiang (Yangtze River) Estuary to the oligotrophic Kuroshio waters and re-evaluation of budgets for the East China Sea Shelf. Prog. Oceanogr. 74 (4), 449–478. https://doi.org/10.1016/j.pocean.2007.04.019.
Zhang, Z., Chen, X.i., Cheng, Q., Li, S., Yue, F., Peng, T., Waldron, S., Oliver, D.M., Soulsby, C., 2020. Coupled hydrological and biogeochemical modelling of nitrogen transport in the karst critical zone. Sci. Total Environ. 732, 138902. https://doi.org/10.1016/j.scitotenv.2020.138902.